Please cite the Published Version

Underlay Spectrum Sharing for NOMA Relaying Networks: Outage Analysis

Sultangali Arzykulov, Galymzhan Nauryzbayev, Theodoros A. Tsiftsis[†], Behrouz Maham, Mohammad S. Hashmi
and Khaled M. Rabie[°]
School of Engineering and Digital Sciences, Nazarbayev University, Nur-Sultan, Kazakhstan
[†]School of Electrical & Information Engineering and the Institute of Physical Internet, Jinan University, China
[°]School of Engineering, Manchester Metropolitan University, Manchester, UK,
Email: {sultangali.arzykulov, galymzhan.nauryzbayev, behrouz.maham, mohammad.hashmi}@nu.edu.kz;
theo_tsiftsis@jnu.edu.cn; k.rabie@mmu.ac.uk

Abstract—**Non-orthogonal multiple access (NOMA) is recognized as a promising multiple access technique for upcoming fifth generation networks and is known for being able to accommodate high system throughput, massive connectivity and low latency. This paper investigates an underlay cognitive radio NOMA network by adopting an amplify-and-forward (AF) relaying method. The end-to-end outage probability (OP) is studied to evaluate the performance of secondary NOMA users. Furthermore, the OP performance for NOMA is compared with conventional orthogonal multiple access to show the supremacy of the former. Moreover, the proposed AF system is compared to the detect-and-forward one. Finally, presented simulation results validate the derived analytical expressions.**

Index Terms—*Amplify-and-forward (AF), cognitive radio (CR), non-orthogonal multiple access (NOMA), outage probability (OP).*

I. INTRODUCTION

Non-orthogonal multiple access (NOMA) has been recently identified as encouraging multiple access (MA) technique for the next fifth generation (5G) wireless networks [1]. Applying NOMA, multiple users are permitted to utilize the whole available resource, e.g., frequency, time, code, etc., and, as a result, the SE of the network can be improved [2]. The power-domain NOMA is the most popular NOMA technique, where multiple users' signals are superimposed at the transmit node with specific power allocation (PA) factors depending on the users' channel quality. For example, to provide users fairness, the transmitter allocates higher power to the users with weak channel conditions, while less power is devoted to the users with strong channel conditions. At the receive side, users with weak channel quality apply successive interference cancellation (SIC) to mitigate the severe effect of interference. In [3], the authors studied the performance of randomly allocated downlink (DL) NOMA users and proved that NOMA is superior to OMA in means of ergodic sum rates. In addition, the authors showed how the outage probability (OP) of the NOMA network can be further improved by an appropriate choice of PA factors. The authors in [2] investigated the OP of the NOMA network with randomly distributed users with partial channel state information (CSI), where the analytical results showed the outperformance of the NOMA network.

Cooperative diversity [4] in wireless networks can be achieved by using dedicated relays which create multiple paths between source and destination nodes to combat fading. It is encouraging to jointly study NOMA networks with relay transmission due to the advantages of both NOMA concept and relay method. Hence, the integration of relay networks with NOMA was studied in [1], [5] where dedicated relay nodes or users can operate as relays to enhance the SE and the transmission reliability of NOMA networks. Moreover, an approximated OP for a cooperative NOMA with the amplify-and-forward (AF) relaying was provided in [6], where it was shown that the proposed network achieves better coding gain compared to the conventional cooperative OMA. Furthermore, exact and asymptotic expressions for the ergodic sum-rate and OP over Nakagami-m fading distributions were derived in [7], where the authors considered multi-user NOMA networks with a variable gain relay which main aim is to maintain the reliable communication between the transmit node and NOMA users.

Cognitive radio (CR) network is a spectrum scarcity resolving technology [8], which consists of two types of users, namely, primary users (PUs) and secondary users (SUs), which can broadcast over the primary spectrum bands. The joint investigation of the CR and NOMA techniques can accommodate further enhancement in effective spectrum utilization. Considering this fact, the underlay CR-NOMA network was investigated in [9], where the secondary transmitter sends a superimposed signal to secondary NOMA destination users. From the results, it was concluded that NOMA users can obtain better performance if the PA factors and target rates are accurately chosen. The authors in [10] derived a closed-form expression for the OP in a DF relaying CR-NOMA and it was concluded that the performance of both PUs and SUs were improved by implementing the NOMA technique. Moreover, underlay CR-NOMA with the DF relaying was studied in [11]. All the above mentioned papers studied the performance of DF CR-NOMA network and no or limited research has been carried out on the AF underlay CR-NOMA.

To the best of our knowledge, cooperative underlay CR-NOMA networks with AF relaying have not been studied yet. Therefore, in this paper, we investigate outage performance and throughput of the dual-hop DL CR-NOMA model with an AF relaying. Furthermore, to avoid harmful interference in the primary network, interference temperature constraint (ITC) is adopted at the primary destination (PD). The main contributions of this paper are summarized as follows:

- We consider the system model with the ITC imposed by the primary receiver node. This assumption is practical

and provides extra useful insights into the system performance. Besides, considering ITC leads to the appearance of an additional random variable (RV), which, in turn, significantly complicates the performance analysis of the system model. In spite of this, we obtain an end-to-end exact OP expression for the proposed system model.

- The impact of the primary interference on the OP of the NOMA secondary destination users is investigated. Moreover, we obtain the PA factors based on the NOMA users' outage fairness (OF) and their channel conditions.
- A good agreement of the theoretical results with Monte Carlo simulations verifies the correctness of our analysis.

II. SYSTEM MODEL

We study a dual-hop CR-NOMA network with underlay paradigm scenario (see Fig. 1), where a secondary source (S) transmits information to two secondary destination users (U_1, U_2) through a half-duplex AF-based secondary relay (R). The channel gains between nodes, i.e., h_{SP}, h_{SR}, h_1 and h_2, are assumed to experience Rayleigh with path-loss exponent η and channel gains are constant withing every transmission block T. The distances between nodes are accordingly given as d_{SP}, d_{SR}, d_1 and d_2. Additionally, the interference from the primary transmitters (PTs) to the secondary users is denoted by I_P[1]. We assume that S can interfere with PD, whereas R can not cause interference to the PUs as it is located far away from PD (see Fig. 1). Hence, S can transmit only if its interference to PD is tolerable. Thus, the transmit power at S is constrained as $P_S \leq \min\left(\frac{P_I d_{SP}^\eta}{|h_{SP}|^2}, \bar{P}_S\right)$, where P_I and $\bar{P}_S$ are the ITC at PD and maximum transmit power available at S, accordingly. Taking into consideration source power restriction, S transmits to R a superimposed signal $\sqrt{P_S} \sum_{i=1}^2 \sqrt{\alpha_i} x_i$, where x_i, with $\mathbb{E}(|x_i|^2) = 1$, is the intended data to U_i, $i \in \{1, 2\}$, while α_i is the PA factor of the respective user's signal, with $\sum_{i=1}^2 \alpha_i = 1$. Furthermore, during time-slot (TS) 1, the received signal at R can be expressed as follows

$$y_R = \sqrt{\frac{P_S}{d_{SR}^\eta}} h_{SR} \sum_{j=1}^2 \sqrt{\alpha_j} x_j + I_P + n_R, \quad (1)$$

where $n_{(\cdot)} \sim \mathcal{CN}(0, \sigma_{(\cdot)}^2)$ denotes the additive white Gaussian noise (AWGN) at each receiver. Hereafter, for mathematical tractability, it is assumed that $\sigma_P^2 = \sigma_R^2 = \sigma_1^2 = \sigma_2^2 = \sigma^2$. We assume that $h_1 < h_2$ and $\alpha_1 > \alpha_2$ which means that S allocates lower power portion to U_2.

In TS 2, based on the AF protocol, R conveys the signal y_R to both secondary destinations. Thus, the received signal at U_i can be written as

$$y_i = \sqrt{\frac{P_S P_R}{d_{SR}^\eta d_i^\eta}} h_{SR} h_i \sum_{j=1}^2 \sqrt{\alpha_j} x_j G$$

[1]Channel conditions of PTs are assumed to be unavailable at the SUs. Hence, regarding to the central limit theorem [12], [13, §3.9.2], interference caused by the PTs to the SUs may be considered as AWGN noise with $\mathcal{CN}(0, \tau\sigma^2)$, where τ is the scaling coefficient of I_P.
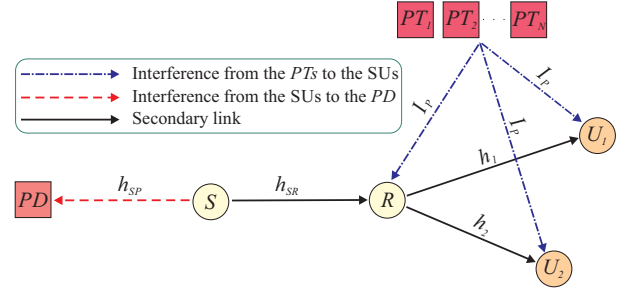

Fig. 1. The proposed system model.

$$+ \underbrace{\sqrt{\frac{P_R}{d_i^\eta}} h_i n_R G + \sqrt{\frac{P_R}{d_i^\eta}} h_i I_P G + I_P + n_i}_{\text{effective noise}}, \quad (2)$$

where G is the amplification factor at R, which can be written as $G = \sqrt{\frac{1}{\frac{P_S}{d_{SR}^\eta}|h_{SR}|^2 + \sigma^2}}$. This yields that U_1, due to higher α_1, can treat x_2 as a noise and detect x_1 by the following signal-to-interference-plus-noise ratio (SINR)

$$\begin{aligned}
\gamma_1 &= \frac{\frac{P_S}{d_{SR}^\eta}|h_{SR}|^2 \frac{P_R}{d_1^\eta}|h_1|^2 G^2 \alpha_1}{\frac{P_S}{d_{SR}^\eta}|h_{SR}|^2 \frac{P_R}{d_1^\eta}|h_1|^2 G^2 \alpha_2 + \frac{P_R}{d_1^\eta}|h_1|^2 G^2 \sigma^2 \bar{\tau} + \sigma^2 \bar{\tau}} \\
&= \frac{n_s Y n_1 X \alpha_1}{n_s Y n_1 X \alpha_2 + n_1 X \bar{\tau} + n_s Y \bar{\tau} + \bar{\tau}}, \quad (3)
\end{aligned}$$

where $\rho_S = \frac{P_S}{\sigma^2}$ and $\rho_R = \frac{P_R}{\sigma^2}$ are the transmit signal-to-noise ratio (SNR) at S and R, respectively; $n_s = \frac{\rho_S}{d_{SR}^\eta}$, $n_1 = \frac{\rho_R}{d_1^\eta}$, $\bar{\tau} = \tau + 1$. $Y = |h_{SR}|^2$ and $X = |h_1|^2$ are the exponential distributions. Next, according to the principle of NOMA [1], U_2 detects x_1, while treating its own signal as a background noise, by the following SINR

$$\begin{aligned}
\gamma_{2,1} &= \frac{\frac{P_S}{d_{SR}^\eta}|h_{SR}|^2 \frac{P_R}{d_2^\eta}|h_2|^2 G^2 \alpha_1}{\frac{P_S}{d_{SR}^\eta}|h_{SR}|^2 \frac{P_R}{d_2^\eta}|h_2|^2 G^2 \alpha_2 + \frac{P_R}{d_2^\eta}|h_2|^2 G^2 \sigma^2 \bar{\tau} + \sigma^2 \bar{\tau}} \\
&= \frac{n_s Y n_2 Q \alpha_1}{n_s Y n_2 Q \alpha_2 + n_2 Q \bar{\tau} + n_s Y \bar{\tau} + \bar{\tau}}, \quad (4)
\end{aligned}$$

where $n_2 = \frac{\rho_R}{d_2^\eta}$ and $Q = |h_2|^2$. After U_2 successfully removes x_1 applying the SIC, it detects its own message x_2 from the remaining signal with the SINR

$$\gamma_2 = \frac{\frac{P_S}{d_{SR}^\eta}|h_{SR}|^2 \frac{P_R}{d_2^\eta}|h_2|^2 G^2 \alpha_2}{\frac{P_R}{d_2^\eta}|h_2|^2 G^2 \sigma^2 \bar{\tau} + \sigma^2 \bar{\tau}} = \frac{n_s Y n_2 Q \alpha_2}{n_2 Q \bar{\tau} + n_s Y \bar{\tau} + \bar{\tau}}. \quad (5)$$

Thus, the achievable rates of U_i can be written as

$$\mathcal{R}_i = \frac{1}{2} \log_2 (1 + \gamma_i,), \quad (6)$$

where $\frac{1}{2}$ indicates the half-duplex relaying.

III. OUTAGE ANALYSIS

The signal of user is assumed to be in outage if the received SNR γ is lower than a predefined threshold $\theta = 2^{2\mathcal{R}_{th}} - 1$,
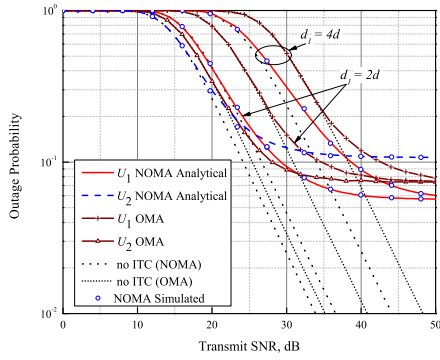
Fig. 2. The OP of Users 1 and 2 vs. the transmit SNR when $\alpha_1 = 0.8$, $\alpha_2 = 0.2$ and $\tau = 0$.

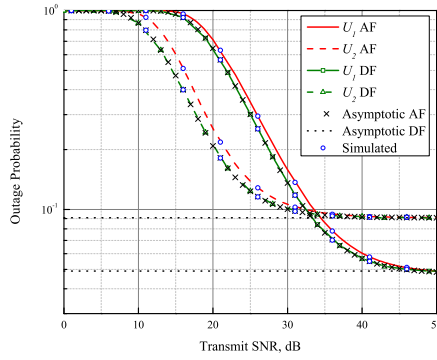
Fig. 3. The OP of Users 1 and 2 vs. the transmit SNR when $d_1 = 3d$, $\alpha_1 = 0.8$, $\alpha_2 = 0.2$ and $\tau = 0$.
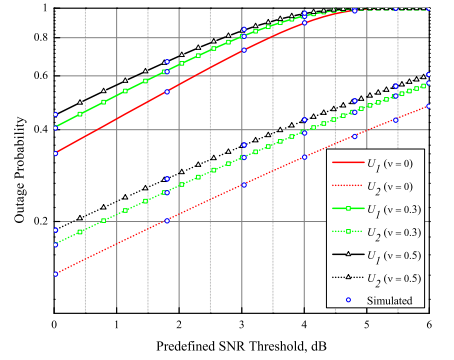

Fig. 4. The OP of Users 1 and 2 vs. the predefined SNR threshold at 20 dB when $d_1 = 3d$.

i.e., $\mathcal{P} = \Pr[\gamma < \theta]$. Thus, the OP of U_1 can be written as

$$\mathcal{P}_1(\theta_1) = 1 - \Pr[\gamma_1 > \theta_1] = 1 - (1 - F_{\gamma_1}(\theta_1)) \triangleq F_{\gamma_1}(\theta_1). \tag{7}$$

Furthermore, considering the ITC, the OP in (7) is derived as in (8), which is shown at the top of the next page, where $\bar{\theta}_1 = \bar{\tau}\theta_1$, $\phi = \alpha_1 - \alpha_2\theta_1$, $n_P = \frac{\rho_I d_{SP}^\eta}{d_{SR}^\eta}$, $c = \frac{\rho_I d_{SP}^\eta}{\rho_S}$, $\rho_I = \frac{P_I}{\sigma^2}$ and $Z = |h_{SP}|^2$. Moreover, the step ε in (8) relies on $\alpha_1 > \alpha_2\theta_1$, otherwise, $\mathcal{P}_1(\theta_1) = 1$ regardless of the system SNR.

Proposition 1: The exact end-to-end OP expression for U_1 is derived as

$$\mathcal{P}_1(\theta_1) = 1 - e^{-\frac{u_1(n_1+n_s)}{n_1}} 2\sqrt{r} K_1(2\sqrt{r})(1 - e^{-c})$$
$$- \frac{n_1 e^{-\frac{cn_1(\bar{u}_1+1)+n_P\bar{u}_1}{n_1}}}{\bar{u}_1(n_p\bar{u}_1+1)} \sum_{k=0}^{\infty} \frac{\left(-\frac{c\bar{u}_1(n_p\bar{u}_1+1)}{n_1}\right)^k}{k!}$$
$$\times G_3^{1\ 3}_2\left(\frac{n_1(\bar{u}_1+1)}{\bar{u}_1(n_p\bar{u}_1+1)} \middle| \begin{array}{ccc} 0, & k-1, & k \\ & 0, & k \end{array}\right). \tag{9}$$

Proof: See Appendix A. ∎

Remark *Proposition 1 shows that the outage of U_1 occurs, i.e., $\mathcal{P}_1(\theta_1) \sim 1$ when $\theta_1 \geq \frac{\alpha_1}{\alpha_2}$. The reason for the outage is that when $\theta_1 \geq \frac{\alpha_1}{\alpha_2}$, the message x_1 is dominated by the interference from the message of U_2 and hence cannot be decoded successfully by U_1. Therefore, Proposition 1 reveals that the minimum transmit power that the source should assign for x_1 is $\frac{P_S\theta_1}{\theta_1+1}$.*

Moreover, the OP for U_2 can be found as

$$\mathcal{P}_2(\theta_2) = 1 - \Pr[\gamma_2 > \theta_2] \triangleq F_{\gamma_2}(\theta_2). \tag{10}$$

Furthermore, using (5), the OP for U_2 can be written as

$$\mathcal{P}_2(\theta_2) = \Pr\left[\frac{n_s Y n_2 Q\alpha_2}{n_2 Q\bar{\tau} + n_s Y\bar{\tau} + \bar{\tau}} < \theta_2, \rho_S < \frac{\rho_I d_{SP}^\eta}{Z}\right]$$
$$+ \Pr\left[\frac{\frac{n_P}{Z} Y n_2 Q\alpha_2}{n_2 Q\bar{\tau} + \frac{n_P}{Z} Y\bar{\tau} + \bar{\tau}} < \theta_2, \rho_S > \frac{\rho_I d_{SP}^\eta}{Z}\right]$$

$$= \underbrace{\Pr\left[Y < \frac{\bar{\theta}_2}{n_s\alpha_2} \triangleq u_2, Q < \frac{Yn_su_2 + u_2}{n_2(Y - u_2)}, Z < c\right]}_{C}$$
$$+ \underbrace{\Pr\left[Y < \frac{Z\bar{\theta}_2}{n_P\alpha_2} \triangleq Z\bar{u}_2, Q < \frac{Yn_P\bar{u}_2 + Z\bar{u}_2}{n_2(Y - Z\bar{u}_2)}, Z > c\right]}_{D}. \tag{11}$$

Now, by following the same approach as in Appendix A, the end-to-end exact OP expression for U_2 is written as

$$\mathcal{P}_2(\theta_2) = 1 - e^{-\frac{u_2(n_2+n_s)}{n_2}} 2\sqrt{r_2} K_1(2\sqrt{r_2})(1 - e^{-c})$$
$$- \frac{n_2 e^{-\frac{cn_2(\bar{u}_2+1)+n_P\bar{u}_2}{n_2}}}{\bar{u}_2(n_p\bar{u}_2+1)} \sum_{k=0}^{\infty} \frac{\left(-\frac{c\bar{u}_2(n_p\bar{u}_2+1)}{n_2}\right)^k}{k!}$$
$$\times G_3^{1\ 3}_2\left(\frac{n_2(\bar{u}_2+1)}{\bar{u}_2(n_p\bar{u}_2+1)} \middle| \begin{array}{ccc} 0, & k-1, & k \\ & 0, & k \end{array}\right), \tag{12}$$

where $r_2 = \frac{u_2(n_su_2+1)}{n_2}$.

IV. NUMERICAL RESULTS AND DISCUSSIONS

The results for the above investigation are presented in this section, which are validated by Monte Carlo simulations. We assume Rayleigh fading channels and adopt the following system parameters: $P_I = 20$ dB, $\alpha_1 = 0.8$, $\alpha_2 = 0.2$, $\theta = 3$ dB[2], $\eta = 2.7$, $d_1 = \{2d, 3d, 4d\}$, $d_{SP} = d_{SR} = d_2 = d$. To focus on the OP results, with no loss of generality, d is assumed to be unity.

The OP results for U_1 and U_2 are shown in Fig. 2. The PA factors are taken as $\alpha_1 = 0.8$ and $\alpha_2 = 0.2$. It is observed that the OP for U_2 performs better than that for U_1 for all d_1 distances. It is due to the fact that U_2 removes the unwanted message of U_1 by applying the SIC technique which improves the probability of errors in the data detection. On the other hand, the OP saturation for U_2 starts at lower SNRs compared with that for U_2. Moreover, it is noticed that the OP of U_1

[2]In the numerical results, we assume an equal predefined SNR threshold for U_1 and U_2, i.e., $\theta_1 = \theta_2 = \theta$, in order to evaluate U_1 and U_2 from the fairness point of view.

$$\mathcal{P}_1(\theta_1) = \Pr\left[\frac{n_s Y n_1 X \alpha_1}{n_s Y n_1 X \alpha_2 + n_1 X \bar{\tau} + n_s Y \bar{\tau} + \bar{\tau}} < \theta_1, \rho_S < \frac{\rho_I d_{SP}^\eta}{Z} \right]$$

$$+ \Pr\left[\frac{\frac{n_P}{Z} Y n_1 X \alpha_1}{\frac{n_P}{Z} Y n_1 X \alpha_2 + n_1 X \bar{\tau} + \frac{n_P}{Z} Y \bar{\tau} + \bar{\tau}} < \theta_1, \rho_S > \frac{\rho_I d_{SP}^\eta}{Z} \right]$$

$$\overset{\varepsilon}{=} \Pr\left[n_1 X \left(n_s Y (\alpha_1 - \alpha_2 \theta_1) - \bar{\theta}_1 \right) < n_s Y \bar{\theta}_1 + \bar{\theta}_1, Z < \frac{\rho_I d_{SP}^\eta}{\rho_S} \right]$$

$$+ \Pr\left[n_1 X \left(\frac{n_p}{Z} Y (\alpha_1 - \alpha_2 \theta_1) - \bar{\theta}_1 \right) < \frac{n_p}{Z} Y \bar{\theta}_1 + \bar{\theta}_1, Z > \frac{\rho_I d_{SP}^\eta}{\rho_S} \right]$$

$$= \underbrace{\Pr\left[Y < \frac{\bar{\theta}_1}{n_s \phi} \triangleq u_1, X < \frac{Y n_s u_1 + u_1}{n_1 (Y - u_1)}, Z < c \right]}_{A} + \underbrace{\Pr\left[Y < \frac{Z \bar{\theta}_1}{n_P \phi} \triangleq Z \bar{u}_1, X < \frac{Y n_P \bar{u}_1 + Z \bar{u}_1}{n_1 (Y - Z \bar{u}_1)}, Z > c \right]}_{B} \quad (8)$$

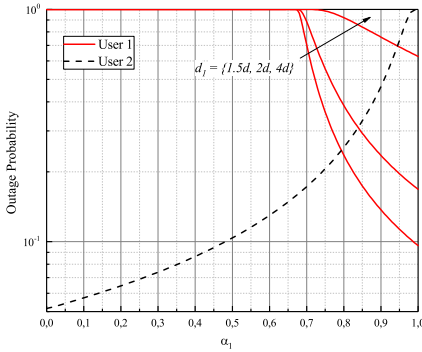
Fig. 5. he OP of Users 1 and 2 vs. the PA factors at 20 dB transmit SNR when $\tau = 0$.
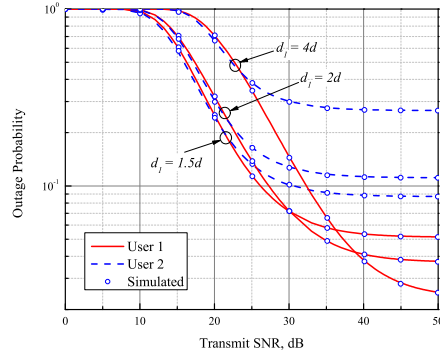
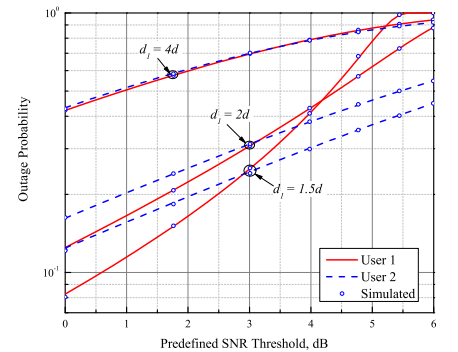Fig. 6. The OP of Users 1 and 2 vs. the transmit SNR considering OF-based PA factors when $\tau = 0$.

Fig. 7. The OP vs. the predefined SNR threshold considering OF-based based PA factors when $\tau = 0$.

degrades as d_1 increases. However, the OP of U_1 starts to saturate at higher SNRs when the value of d_1 increases. This phenomenon can be explained by the fact that higher α_1 is required when U_1 is located farther from R. Moreover, Fig. 2 also compares the OP results derived for NOMA with simulated results of OMA in the cases without ITC, i.e., $P_I = \infty$, and when $P_I = 20$ dB. The proposed AF-based CR-NOMA needs two TSs to transmit NOMA messages, while cooperative OMA uses four TSs to serve the same number of users. Thus, for a fair comparison, we set the data requirements for CR-OMA as bi-fold of that for CR-NOMA.

In addition to this, we assume that the source and the relay transmit power levels are normalized to P. Therefore, in the OMA system, each transmit node allocates power of $\frac{1}{2}P$ for each data transmission. The rest parameters of the CR-OMA system remain the same as those of the CR-NOMA system mentioned above. In Fig. 2, within no ITC regime, both NOMA users outperform the OMA users in terms of the OP for all SNR values. However, when the ITC is applied ($P_I = 20$ dB), OMA users' OP curves start their saturation at higher SNR levels compared with NOMA users' OP ones. It is due to the fact that, regarding transmit power constraint, the ITC level at the primary network is increased due to the transmitted power of $\frac{1}{2}P$ by secondary users.

In Fig. 3, the OP is plotted versus the transmit SNR for U_1 and U_2 when $d_1 = 3d$. We compare the OP of the proposed AF mode with that of the DF mode presented in [14]. Moreover, the approximated OP results for both AF and DF modes are also plotted, where we used an approximation of $e^{-t} = 1 - t$ and $K_1(\omega) \sim 1/\omega$ for high SNR regimes. It can be observed from the plot that the DF relaying performs better than the AF one. Furthermore, the OP of the high SNR approximation of the AF mode is consistent with that of the DF mode, which means that the maximum optimal OP of the AF can not exceed the outage performance of the DF mode. In addition, Monte Carlo simulations results agree with the derived analytical results, which confirm the accuracy of the analytical exact and approximated OP expressions.

Fig. 4 illustrates the results of the OP versus the predefined SNR threshold in the cases when $\tau = \{0, 0.3, 0.5\}$. The observation is that the OP degrades as the predefined SNR threshold value increases. Moreover, the OP for U_2 performs better compared to that for U_1. Thus, due to the remoteness of U_1 from R (compared to the R - U_2 distance), the OP of x_1 degrades dramatically after 3.5 dB. in addition, it was noticed that the primary interference degrades the performance of the SUs. For example, when no primary interference exist, U_1 is in an outage at about 5 dB, while, with the PN interference,

Table I. The OF-based PA factors.

d_1	$1.5d$	$2d$	$4d$
α_1	0.79	0.84	0.945
α_2	0.21	0.16	0.055

outage for U_1 starts at about 4.6 dB.

The numerical results on the OF-based PA factors for NOMA users are shown in Fig. 5. It is noted that, when $\theta_1 > \frac{\alpha_1}{\alpha_2}$, User 1 is always in an outage, i.e., $\mathcal{P}_1 = 1$, for all d_1 values. When $\theta_1 < \frac{\alpha_1}{\alpha_2}$, an increase of α_1 helps improve the outage performance of User 1. On the other hand, an increase of α_1 degrades the OP of User 2. It is also noticed that when α_1 approaches 1, User 2 is in outage, while User 1 obtains the best outage performance. This is due to the fact that User 1 is allocated with the maximum transmit power. Table I illustrates all observed values of the OF-based PA factors.

Fig. 6 illustrates the OP versus the transmit SNR with the OF-based (α_1) and (α_2) regarding different d_1. It is observed from the figure that, for all d_1 values, User 2 shows better outage performance compared to User 1 at lower SNRs (< 22 dB). However, at higher SNR levels, User 1 is superior to User 2 in terms of the outage performance. Furthermore, when the value of d_1 rises, the OP saturation of User 1 commences at higher SNR levels. This is due to the fact that User 1 requires a larger value of α_1 when it is located farther from R. Finally, at about 22 dB, the OP difference of both users is the same, which confirms that OF-based PA factors provide the OP fairness for NOMA users.

Fig. 7 illustrates the results on the OP versus the predefined SNR threshold considering the OF-based PA factors for various d_1 at 20 dB transmit SNR. It is worth mentioning that the OF-based (α_1) and (α_2) improve the outage performance of User 1 (for all d_1 values) and provide fairness among NOMA users, especially, at the predefined SNR threshold of 3 dB.

V. CONCLUSION

In this paper, we studied the OP of the underlay CR-NOMA AF relaying network. Exact end-to-end OP expressions for the secondary NOMA users were derived and compared to those of the corresponding OMA system. The comparison result indicated that the cooperative CR-NOMA is obviously superior to the cooperative CR-OMA. Moreover, it was shown that properly evaluated PA factors guarantee the OP fairness among NOMA users. Furthermore, the derived OP results for the AF mode were compared to those for the DF one. All derived analytical results were validated by the Monte Carlo simulations. In future work, multiple numbers of CR-NOMA users with wireless power transfer capability will be considered, where both secondary source and relay cause interference to primary networks.

APPENDIX A
PROOF OF PROPOSITION 1

The term A in (8) can be further extended as

$$
A = \underbrace{\int_0^c f_Z(z)\mathrm{d}z \int_0^{u_1} f_Y(y)\mathrm{d}y}_{A_1}
$$
$$
+ \underbrace{\int_0^c f_Z(z)\mathrm{d}z}_{A_2} \underbrace{\int_{u_1}^{\infty} F_X\left(\frac{yn_s u_1 + u_1}{n_1(y - u_1)}\right) f_Y(y)\mathrm{d}y}_{A_3}, \quad (13)
$$

where $f_{(\cdot)}(\cdot)$ and $F_{(\cdot)}(\cdot)$ denote the probability density function (PDF) and cumulative distribution function (CDF), respectively. The PDFs in the term A_1 are independent from each other, thus, the term A_1 can be written as

$$
A_1 = \int_0^c f_Z(z)\mathrm{d}z \int_0^{u_1} f_Y(y)\mathrm{d}y = \left(1 - e^{-c}\right)\left(1 - e^{-u_1}\right), \quad (14)
$$

while A_2 can be written as

$$
A_2 = \int_0^c f_Z(z)\mathrm{d}z = \left(1 - e^{-c}\right). \quad (15)
$$

Then, the term A_3 in (13) can be further extended as

$$
A_3 = \underbrace{\int_{u_1}^{\infty} e^{-y}\mathrm{d}y}_{A_{31}} - \underbrace{\int_{u_1}^{\infty} e^{-\frac{yn_s u_1 + u_1}{n_1(y - u_1)} - y}\mathrm{d}y}_{A_{32}}. \quad (16)
$$

The term A_{31} in (16) can be further rewritten as

$$
A_{31} = \int_{u_1}^{\infty} e^{-y}\mathrm{d}y = e^{-u_1}. \quad (17)
$$

Moreover, by substituting $t_1 = y - u_1$, A_{32} in (16) can be rewritten as follows

$$
A_{32} = \int_0^{\infty} e^{-\frac{t_1 n_s u_1 + n_s u_1^2 + u_1}{n_1 t_1} - t_1 - u_1}\mathrm{d}t_1
$$
$$
= e^{-\frac{u_1(n_1 + n_s)}{n_1}} \int_0^{\infty} e^{-\frac{u_1(n_s u_1 + 1)}{n_1}\frac{1}{t_1} - t_1}\mathrm{d}t. \quad (18)
$$

Then, using [15, Eq. (3.324.1)], A_{32} can be further derived as

$$
A_{32} = e^{-\frac{u_1(n_1 + n_s)}{n_1}} 2\sqrt{\frac{u_1(n_s u_1 + 1)}{n_1}} K_1\left(2\sqrt{\frac{u_1(n_s u_1 + 1)}{n_1}}\right), \quad (19)
$$

where $K_1(\cdot)$ is the modified Bessel function of the second kind of order 1. Further, the term A, after substituting (14), (15), (17) and (19) into (13) is reformulated as

$$
A = \left(1 - e^{-c}\right)\left(1 - e^{-u_1}\right) + \left(1 - e^{-c}\right)
$$
$$
\times \left(e^{-u_1} - e^{-\frac{u_1(n_1 + n_s)}{n_1}} 2\sqrt{r_1} K_1\left(2\sqrt{r_1}\right)\right)
$$
$$
= \left(1 - e^{-c}\right)\left(1 - e^{-\frac{u_1(n_1 + n_s)}{n_1}} 2\sqrt{r_1} K_1\left(2\sqrt{r_1}\right)\right), \quad (20)
$$

where $r_1 = \frac{u_1(n_s u_1 + 1)}{n_1}$.

Now, we further extend the term B in (8) by

$$B = \underbrace{\int_c^\infty f_Z(z) \int_0^{z\bar{u}_1} f_Y(y)\mathrm{d}y\mathrm{d}z}_{B_1}$$
$$+ \underbrace{\int_c^\infty f_Z(z) \int_{z\bar{u}_1}^\infty f_Y(y) F_X\left(\frac{n_p y \bar{u}_1 + z\bar{u}_1}{n_1(y - z\bar{u}_1)}\right)\mathrm{d}y\mathrm{d}z}_{B_2}.$$
(21)

The term B_1 in (21) can be derived as

$$B_1 = \int_c^\infty e^{-z} \int_0^{z\bar{u}_1} e^{-y}\mathrm{d}y\mathrm{d}z = \int_c^\infty e^{-z}\left(1 - e^{-z\bar{u}_1}\right)\mathrm{d}z$$
$$= \int_c^\infty e^{-z}\mathrm{d}z - \int_c^\infty e^{-z(\bar{u}_1+1)}\mathrm{d}z = e^{-c} - \frac{e^{-c(\bar{u}_1+1)}}{\bar{u}_1 + 1}.$$
(22)

Further, the term B_2 in (21) can be rewritten as

$$B_2 = \int_c^\infty e^{-z}\left(\int_{z\bar{u}_1}^\infty e^{-y}\mathrm{d}y - \underbrace{\int_{z\bar{u}_1}^\infty e^{-\frac{n_p y\bar{u}_1 + z\bar{u}_1}{n_1(y - z\bar{u}_1)} - y}\mathrm{d}y}_{B_{21}}\right)\mathrm{d}z.$$
(23)

Then, by using substitution $p_1 = y - z\bar{u}_1$ and [15, Eq. (3.324.1)], the term B_{21} in (23) is derived by

$$B_{21} = \int_0^\infty e^{-\frac{n_p \bar{u}_1 p_1 + n_p \bar{u}_1^2 z + z\bar{u}_1}{n_1 p_1} - p_1 - z\bar{u}_1}\mathrm{d}p_1$$
$$= e^{-\frac{\bar{u}_1(n_p + zn_1)}{n_1}} \int_0^\infty e^{-\frac{z\bar{u}_1(n_p\bar{u}_1 + 1)}{n_1 p_1} - p_1}\mathrm{d}p_1$$
$$= e^{-\frac{\bar{u}_1(n_p + zn_1)}{n_1}} 2\sqrt{s_1} K_1\left(2\sqrt{s_1}\right),$$
(24)

where $s_1 = \frac{z\bar{u}_1(n_p\bar{u}_1 + 1)}{n_1}$. Now, we rewrite (23) using (24) as

$$B_2 = \int_c^\infty e^{-\bar{u}_1 z - z}\mathrm{d}z - \int_c^\infty e^{-\frac{\bar{u}_1(n_p + zn_1)}{n_1} - z}$$
$$\times 2\sqrt{s_1} K_1(2\sqrt{s_1})\mathrm{d}z = \frac{e^{-c(\bar{u}_1+1)}}{\bar{u}_1 + 1}$$
$$- \underbrace{\int_c^\infty e^{-\frac{zn_1(\bar{u}_1+1) + n_p\bar{u}_1}{n_1}} 2\sqrt{s_1} K_1(2\sqrt{s_1})\mathrm{d}z}_{B_{22}}.$$
(25)

Then, substituting $q = z - c$ and after some algebraic manipulations, the term B_{22} in (25) can be rewritten as

$$B_{22} = e^{-\frac{cn_1(\bar{u}_1+1) + n_p\bar{u}_1}{n_1}}$$
$$\times \underbrace{\int_0^\infty e^{-q(\bar{u}_1+1)} 2\sqrt{l_1} K_1\left(2\sqrt{l_1}\right)\mathrm{d}q}_{\Lambda}.$$
(26)

where $l_1 = \frac{q\bar{u}_1(n_p\bar{u}_1 + 1) + c\bar{u}_1(n_p\bar{u}_1 + 1)}{n_1}$. Further, after applying [16, Eqs. (12) and (14)] and [17, Eq. (2.24.1.3)] to Λ in (26) and by substituting (22) - (25) into (21), the term B can be

written as

$$B = e^{-c} - \frac{n_1 e^{-\frac{cn_1(\bar{u}_1+1) + n_p\bar{u}_1}{n_1}}}{\bar{u}_1(n_p\bar{u}_1 + 1)} \sum_{k=0}^\infty \frac{\left(-\frac{c\bar{u}_1(n_p\bar{u}_1 + 1)}{n_1}\right)^k}{k!}$$
$$\times G_{3\ 2}^{1\ 3}\left(\frac{n_1(\bar{u}_1 + 1)}{\bar{u}_1(n_p\bar{u}_1 + 1)} \left|\begin{array}{ccc} 0, & k-1, & k \\ 0, & k & \end{array}\right.\right)$$
(27)

Finally, the exact OP expression for U_1 is derived by substituting (20) and (27) into (8) and written as in (9), where $\theta_1 < \frac{\alpha_1}{\alpha_2}$, otherwise, $\mathcal{P}_1(\theta_1) \sim 1$, which completes the proof. ∎

REFERENCES

[1] Z. Ding, M. Peng, and H. V. Poor, "Cooperative non-orthogonal multiple access in 5G systems," *IEEE Communications Letters*, vol. 19, pp. 1462–1465, Aug. 2015.

[2] Z. Yang, Z. Ding, P. Fan, and G. K. Karagiannidis, "On the performance of non-orthogonal multiple access systems with partial channel information," *IEEE Transactions on Communications*, vol. 64, pp. 654–667, Feb. 2016.

[3] Z. Ding, Z. Yang, P. Fan, and H. V. Poor, "On the performance of non-orthogonal multiple access in 5G systems with randomly deployed users," *IEEE Signal Processing Letters*, vol. 21, pp. 1501–1505, Dec. 2014.

[4] J. N. Laneman, D. N. C. Tse, and G. W. Wornell, "Cooperative diversity in wireless networks: Efficient protocols and outage behavior," *IEEE Transactions on Information Theory*, vol. 50, pp. 3062–3080, Dec. 2004.

[5] C. Y. Ho and C. Y. Leow, "Cooperative non-orthogonal multiple access using two-way relay," in *2017 IEEE International Conference on Signal and Image Processing Applications (ICSIPA)*, pp. 459–463, Sep. 2017.

[6] X. Liang *et al.*, "Outage performance for cooperative NOMA transmission with an AF relay," *IEEE Communications Letters*, vol. 21, pp. 2428–2431, Nov. 2017.

[7] J. Men, J. Ge, and C. Zhang, "Performance analysis of nonorthogonal multiple access for relaying networks over Nakagami-m fading channels," *IEEE Transactions on Vehicular Technology*, vol. 66, pp. 1200–1208, Feb. 2017.

[8] A. Goldsmith *et al.*, "Breaking spectrum gridlock with cognitive radios: An information theoretic perspective," *Proceedings of the IEEE*, vol. 97, pp. 894–914, May 2009.

[9] Y. Liu, Z. Ding, M. Elkashlan, and J. Yuan, "Nonorthogonal multiple access in large-scale underlay cognitive radio networks," *IEEE Transactions on Vehicular Technology*, vol. 65, pp. 10152–10157, Dec. 2016.

[10] L. Lv, J. Chen, Q. Ni, and Z. Ding, "Design of cooperative non-orthogonal multicast cognitive multiple access for 5G systems: User scheduling and performance analysis," *IEEE Transactions on Communications*, vol. 65, pp. 2641–2656, Jun. 2017.

[11] S. Lee, T. Q. Duong, D. B. da Costa, D. Ha, and S. Q. Nguyen, "Underlay cognitive radio networks with cooperative non-orthogonal multiple access," *IET Communications*, vol. 12, no. 3, pp. 359–366, 2018.

[12] S. Arzykulov, T. A. Tsiftsis, G. Nauryzbayev, and M. Abdallah, "Outage performance of cooperative underlay CR-NOMA with imperfect CSI," *IEEE Communications Letters*, vol. 23, pp. 176–179, Jan. 2019.

[13] T. Q. S. Quek, G. Roche, I. Guvenc, and M. Kountouris, *Deployment, PHY Techniques, and Resource Management*. Cambridge University Press, UK, 2013.

[14] S. Arzykulov, T. A. Tsiftsis, G. Nauryzbayev, M. Abdallah, and G. Yang, "Outage performance of underlay CR-NOMA networks with detect-and-forward relaying," in *2018 IEEE Global Communications Conference (GLOBECOM)*, pp. 1–6, Dec. 2018.

[15] I. S. Gradshteyn and I. M. Ryzhik, *Table of Integrals, Series, and Products*. A. Jeffrey, Ed. San Diego: Academic Press, 2000.

[16] V. S. Adamchik and O. I. Marichev, "The algorithm for calculating integrals of hypergeometric type functions and its realization in reduce system," in *International Conference on Symbolic and Algebraic Computation*, pp. 212–224, 1990.

[17] A. P. Prudnikov, Y. A. Brychkov, and O. I. Marichev, *Integrals and Series, Vol. 3: More Special Functions*. Gordon and Breach, New York, 1990.